Back-scattering of Fast Protons from Silicon Single Crystals

AUTHOR(S):

SONE, Kazuho; NATSUAKI, Nobuyoshi; FUKUZAWA, Fumio

CITATION:

SONE, Kazuho ...[et al]. Back-scattering of Fast Protons from Silicon Single Crystals. Memoirs of the Faculty of Engineering, Kyoto University 1971, 33(3): 174-185

ISSUE DATE:

1971-09-30

URL:

http://hdl.handle.net/2433/280853

Back-scattering of Fast Protons from Silicon Single Crystals

By

Kazuho SONE, Nobuyoshi NATSUAKI and Fumio FUKUZAWA

(Received March 30, 1971)

The ⟨111⟩ axial and (110) planar channeling of 200 keV protons in silicon have been studied by measuring the yield of back-scattering (scattering angle: 135°). The results are in good agreement with the theory of Lindhard and Erginsoy. The observed critical angles and the minimum scattering yield agree with the theoretical values with decreasing depth below the crystal surface. The analysis of the energy spectra of back-scattered protons indicates that the axial and planar channeling probabilities of the protons at the clean surface are 0.93 and 0.66, respectively, and that the shoulder parts of the yield curves are mainly due to back-scattering from the surface layer of the crystal rather than to some imperfections of its surface.

1. Introduction

Since experimental evidence of charged particle channeling were shown in 1963 by Piercy et al.,[1] Nelson et al.,[2] and Lutz et al.,[3] many experiments have been done both in axial and planar effects. These are divided into three types; charged particle transmission through thin single crystal foils, production of characteristic radiations or nuclear reactions, and wide-angle Rutherford scattering from thick single crystal targets. The present study belongs to the third type. Recently, experiments of this type have been done by several investigators.[4-10]

The Rutherford scattering yield may be greatly reduced when the energetic charged particles enter the crystal within a certain critical angle of a low-index axis or plane. In experimental studies of channeling mechanism, back-scattering is expected to have several advantages over the other methods. In particular, from an analysis of the energy spectra of the back-scattered particles, the scattering process of the channeled particles can be studied at a given depth below the surface of the thick target.

The analysis of the energy spectra of the channeled particles has been made very frequently in many experiments of particle transmission, but in experiments of

Department of Nuclear Engineering

Rutherford scattering, there have been only qualitative descriptions because of relatively insufficient knowledge of the orientation dependence of the stopping power. In this paper is shown from the energy analysis such important information as the channeling probability and the hump in the energy spectrum of back-scattered protons.

Lindhard[11] has developed extensively a classical theory of channeling. In **4**, the observed critical angles and the minimum scattering yield are compared with his predictions.

2. Experimental Procedures

A schematic diagram of the experimental arrangement is shown in Fig. 1. The beam of 200 kev protons from the Cockcroft-Walton accelerator was collimated by two identical slits, each having a 1.0 mm diameter hole. The two slits were one meter apart, and then the beam divergence was limited to within 0.12°. A small piece of silicon single crystal, about 50 μm thick, was glued to a copper plate which was supported by an insulating teflon cylinder. The crystal surface was almost parallel to a (111) plane. In order to change the crystal orientation with

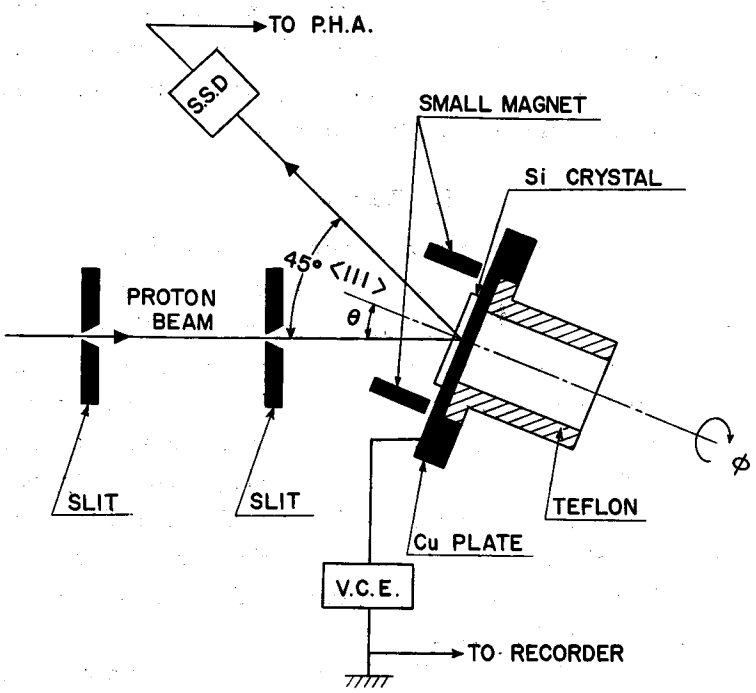

Fig. 1. Schematic diagram of the experimental arrangement. The axis of rotation (*i.e.* ϕ-axis) and the incident beam axis are expected to be on the same horizontal plane.

respect to the direction of the incident beam, the tilting angle θ and the rotating angle ϕ of the goniometer were adjusted independently as shown in Fig. 1, with accuracy of 0.025°. The most essential point is that the axis of rotation (i.e. ϕ-axis) and the incident beam axis crossed at the target surface. In the present case, these axes were expected to be almost on the same horizontal plane. The goniometer with some bearings and O-ring seals was fixed to the upper lid of the scattering chamber, and θ and ϕ could be varied smoothly in the vacuum.

The back-scattering yield was measured by a solid-state detector placed about 10 cm apart from the beam spot on the crystal surface. The energy resolution of the detecting system was approximately 10 keV for 200 keV protons. The detector had an opening angle of 0.0075 steradians. The scattering angle was 135°. The beam current to the crystal target was measured with a vibrating capacitor electrometer (V.C.E.), and kept to the order of 1 nA. A small magnet, whose field strength was about 35 G at the center of the gap, was placed in front of the target in order to return secondary electrons emitted from the target by proton impact. The bombarded area of the target was about 0.05 cm^2.

The energy spectra of the scattered protons were analysed with a 256-channel pulse height analyser (P.H.A.). The accurate orientation of the single crystal target to the incident beam axis was determined by measuring the variation of Rutherford scattering yields for the continuously varied rotating angle ϕ.[12,13] The scattering chamber was evacuated to pressure of 10^{-6} mmHg.

3. Results

Fig. 2 illustrates the energy spectra for aligned and random directions. The scattering yield for $\langle 111 \rangle$ axial and (110) planar directions decreases in the whole energy range in comparison with that for random directions.

Fig. 3 shows the directional dependence of the scattering yield. It is normalized at $\theta = -8.1°$ of a random direction in the $\langle 111 \rangle$ axial case, and similarly at $\phi = -11.7°$ in the (110) planar case. An extremely strong reduction (about a factor of 10 and 2 for axial and planar channeling, respectively) is observed when the proton beams enter the crystal within a small angle of the close-packed $\langle 111 \rangle$ axes or (110) planes. In both cases, the shoulder parts are clearly observed. It should be noted that energy spectra in these parts have the humps near the maximum energy (see Fig. 2).

The results shown in Fig. 2 and Fig. 3 indicate that proton channeling occurs strongly both in the $\langle 111 \rangle$ axial and (110) planar directions of a silicon single crystal.

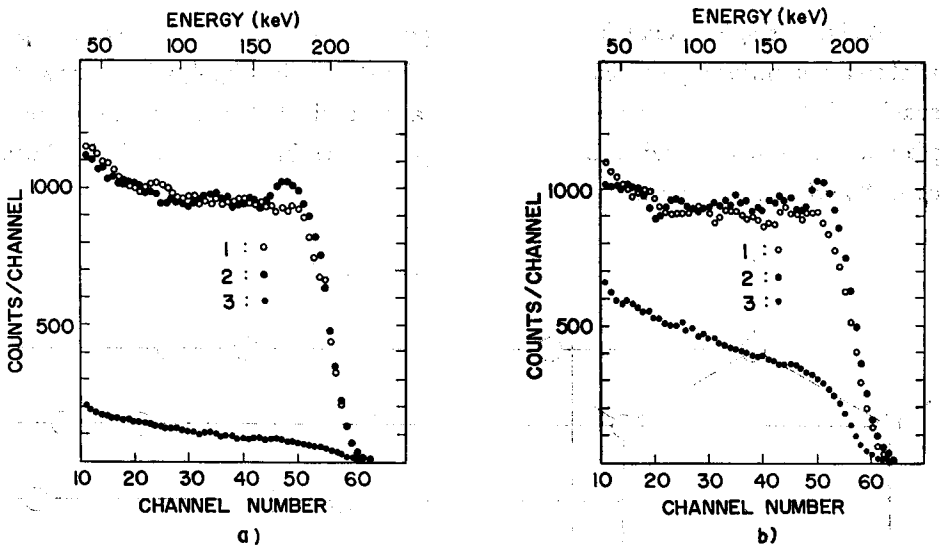

Fig. 2. Energy spectra of protons back-scattered from a silicon single crystal at room temperature (15°C). a) 1: along a random direction ($\theta = -5.85°$), 2: at the shoulder part ($\theta = -4.35°$), 3: almost parallel to a <111> axis. b) 1: along a random direction ($\phi = -11.7°$); , 2: at the shoulder part ($\phi = -5.0°$), 3: almost parallel to a (110) plane. Total incident charge: 50 nC. Incident proton energy: 200 keV.

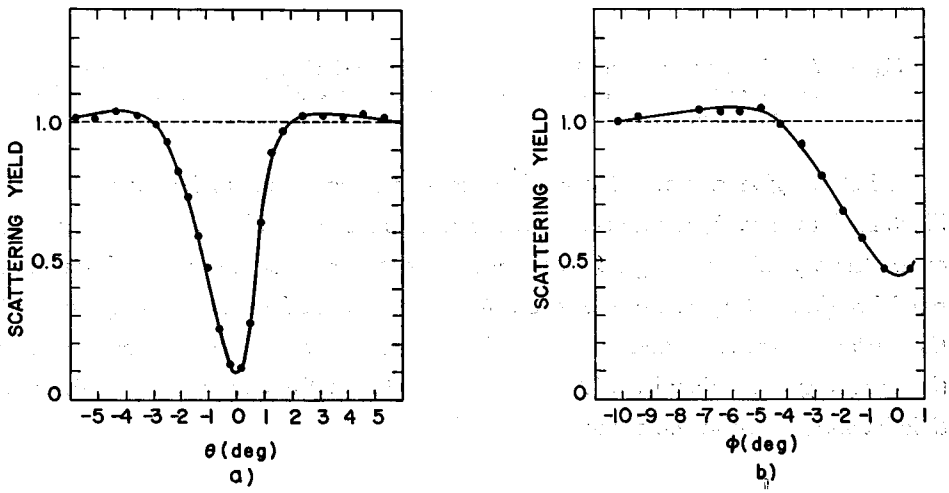

Fig. 3. Directional dependence of the scattering yield of 200 keV protons in the vicinity of a) <111> axial and b) (110) planar directions of the silicon crystal.

4. Discussions

A silicon single crystal has diamond-type lattices. The ⟨111⟩ axes are parallel to a nonuniformly spaced atomic row as illustrated in Fig. 4, which shows the spacing between the atoms along ⟨111⟩ axes and that between neighboring planes. Channeling studies in diamond-type lattices have been made by Sattler et al.[14] and Picraux et al..[8]

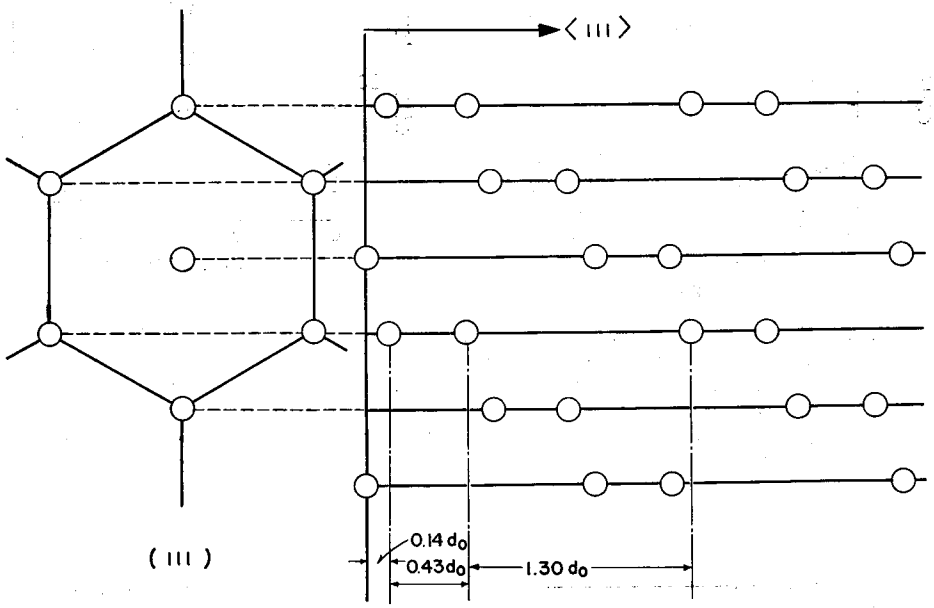

Fig. 4. Atomic positions in the (110) plane of the silicon single crystal lattice. The ⟨111⟩ axial directions are parallel to a nonuniformly spaced atomic row. d_0: lattice constant (5.43 Å).

First we give a model for Rutherford scattering of channeled particles. As illustrated in Fig. 5, a monoenergetic beam (particle mass M_1 and energy E_p) enters the crystal at an angle θ_1 with respect to the surface normal, and scattered particles (laboratory scattering angle θ_s) leave the surface at an angle θ_2 with the surface normal. When the incoming trajectory is parallel to channels and the outgoing one coincides with a random direction, the energy E_{obs} of the particle back-scattered at the depth x is given by

$$E_{obs} = k^2\left[E_p - \int_0^{x_1} S^*(E)\mathrm{d}x_1\right] - \int_0^{x_2} S(E)\mathrm{d}x_2\,, \qquad (1)$$

where k is the fractional energy-loss in elastic scattering:

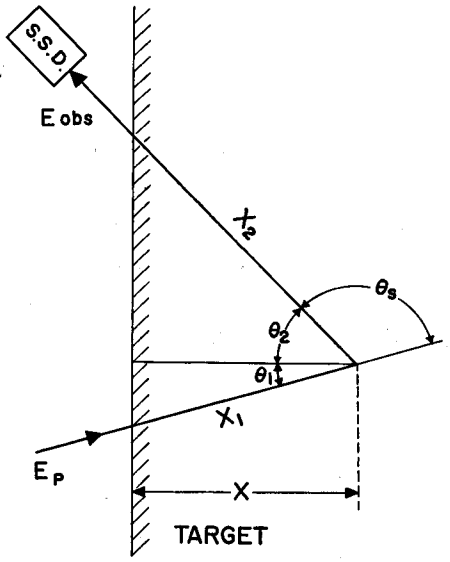

Fig. 5. Schematic diagram of back-scattering of channeled protons.

$$k = \frac{M_1 \cos\theta_s}{M_1+M_2} + \left[\left(\frac{M_1 \cos\theta_s}{M_1+M_2}\right)^2 + \frac{M_2-M_1}{M_1+M_2}\right]^{1/2}, \tag{2}$$

and $S^*(E)$ and $S(E)$ are the stopping powers for the aligned and random beams, respectively. In addition, x_1 and x_2 are the distances along the incoming and outgoing trajectories, respectively, and then $x_1=x/\cos\theta_1$, and $x_2=x/\cos\theta_2$. From eq. (1) the following relationship is derived:

$$x(E_{obs}) = (k^2E_p - E_{obs}) \Big/ \left[\frac{k^2\langle S^*\rangle_{av}}{\cos\theta_1} + \frac{\langle S\rangle_{av}}{\cos\theta_2}\right]. \tag{3}$$

Since the specific energy-loss of protons in polycrystalline silicon is nearly constant over the relatively wide range of energy around 200 keV, the dependence of $\langle S^*\rangle_{av}$ and $\langle S\rangle_{av}$ on x is not strong. The quantity in the square bracket in eq. (3) may be regarded approximately as constant. Therefore, the following quantity ΔE may be used as a good measure of the scattering depth x:

$$\Delta E = k^2E_p - E_{obs}\,. \tag{4}$$

4.1. The Critical Angle

According to the classical theory of Lindhard,[11] the critical angles θ_c and ϕ_c are given by

$$\theta_c(d) = C'\left(\frac{2Z_1Z_2e^2}{dE}\right)_{1/2} \qquad \text{for} \quad E>E' = 2Z_1Z_2e^2d/a_{TF}^2\,, \tag{5}$$

and

$$\phi_c = C'\left(\frac{\theta_c^*}{2Z_2^{1/6}}\right), \quad \theta_c^* = \theta_c(\bar{d}) . \tag{6}$$

Here Z_1 and Z_2 are the atomic numbers of the incident particles and the target atoms, respectively, e is the electronic charge, d the spacing between the atoms along the chosen axis and C' a constant approximately 1.5–2.0. In eq. (6) θ_c^* is the characteristic angle of an axis having the same mean lattice spacing $\bar{d}$ as the plane. Hence, $\bar{d} = (d_p N)^{-1/2}$, where d_p is the spacing between the chosen lattice planes and N is the atomic number density per cm^3. The Thomas-Fermi screening distance a_{TF} is given by

$$a_{TF} = 0.8853 a_0 (Z_1^{2/3} + Z_2^{2/3})^{-1/2} , \tag{7}$$

where a_0 is the Bohr radius, $a_0 = 0.529$ Å.

On the other hand, Erginsoy[16] has derived the critical angle ψ_c both in axial and planar channeling as follows:

$$\psi_c = \left(\frac{U(a_{TF})}{E}\right)^{1/2}, \tag{8}$$

where $U(r)$ is the average string or plane potential. According to the Molière's approximation to Thomas-Fermi potential, $U(r)$ is given by

$$U(r) = (2Z_1 Z_2 e^2/d)[0.1K_0(6r/a_{TF}) + 0.55K_0(1.2r/a_{TF}) + 0.35K_0(0.3r/a_{TF})] \quad \text{for axial,} \tag{9}$$

or

$$U(r) = (2\pi Z_1 Z_2 e^2 a_{TF}/A)\left[\frac{0.1}{6}\exp(-6r/a_{TF}) + \frac{0.55}{1.2}\exp(-1.2r/a_{TF}) + \frac{0.35}{0.3}\exp(-0.3r/a_{TF})\right] \quad \text{for planar,} \tag{10}$$

where r is the distance to the axis or plane and $K_0(z)$ the zero-order modified Bessel function of the second kind.

In the above-mentioned treatment, the lattice vibration is neglected. Davies et al.,[15] have shown that the value of C' is approximately unity in conformity with the experimental results for real lattices. In silicon, they concluded that $C' = 1.125$. In Table I are shown the critical angles θ_c and ϕ_c for 200 keV protons estimated from eqs. (5)–(10) for $C' = 1.0$ and $C' = 1.125$. From Fig. 3, the observed values of θ_c and ϕ_c $1.0° \pm 0.2°$ and $2.2° \pm 0.2°$, respectively.

Fig. 6 shows the depth dependence of the scattering yield curve. The specific

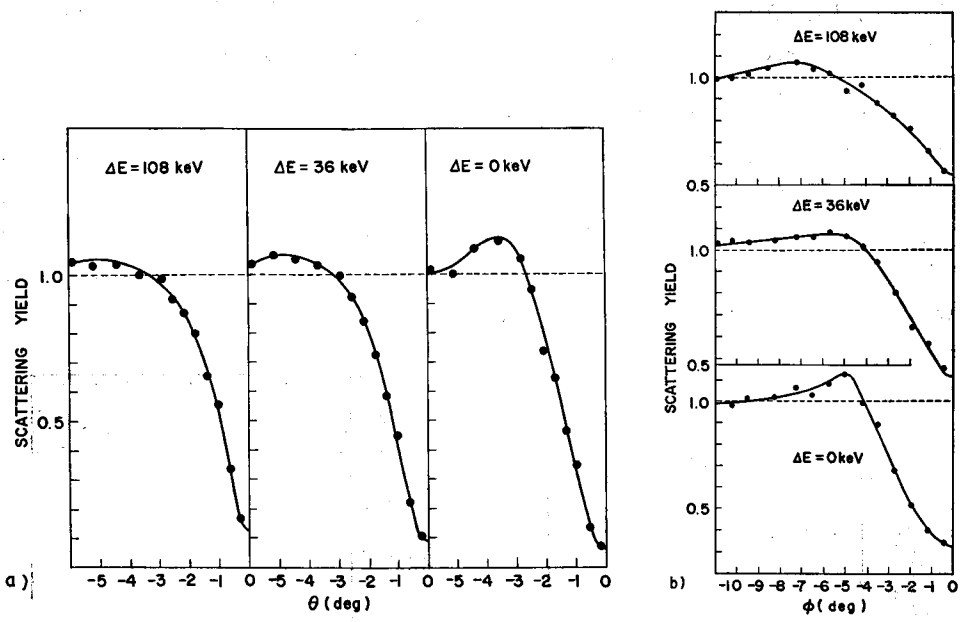

Fig. 6. Depth dependence of the scattering yield curve in silicon in the vicinity of a) ⟨111⟩ axial and b) (110) planar directions. The energy-loss ΔE is taken as a depth scale.

energy-loss of channeled protons is unknown, so that the depth dependence is expressed as a function of the energy-loss ΔE on the basis of eq. (3). That is to say, the scattering depth below the crystal surface increases with increasing ΔE. The variation of θ_c and ϕ_c as a function of ΔE is illustrated in Fig. 7. This result may suggest that the critical angles increase exponentially with decreasing depth. The extrapolated values of the critical angles of θ_c and ϕ_c at $\Delta E=0$ are

Table I. a) Critical angles θ_c for ⟨111⟩ axial channeling.

	Theoretical		Experimental
	$C'=1.0$	$C'=1.125$	
Lindhard	1.19°	1.34°	1.2°±0.1°
Erginsoy	1.36°	1.53°	

Table I. b) Critical angles ϕ_c for (110) planar channeling.

	Theoretical		Experimental
	$C'=1.0$	$C'=1.125$	
Lindhard	0.49°	0.55°	0.65°±0.05°
Erginsoy	0.61°	0.69°	

given by θ_c(experimental) $=1.2°\pm0.1°$and ϕ_c(observed) $=2.5°\pm0.2°$, respectively. The value of ϕ_c(experimental) is derived from the following correction:

$$\phi_c(\text{experimental}) = \phi_c(\text{observed}) \sin\theta \,. \tag{11}$$

We fixed the tilting angle θ to be $15.0°\pm0.1°$, and then we obtain ϕ_c(experimental) $=0.65°\pm0.05°$. On the other hand, the theoretical values of the critical angles predicted by Lindhard[11] and Erginsoy[16] are shown in Table I together with the experimental values. Thus, the theory of Lindhard and Erginsoy describe well the channeling phenomena at the surface layer of the crystal.

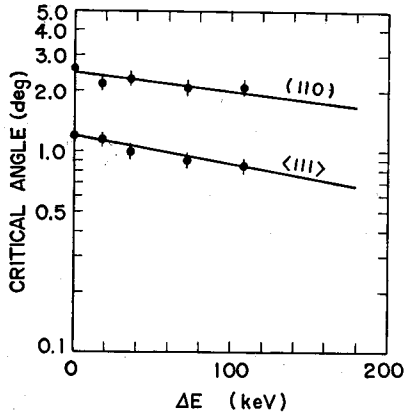

Fig. 7. Depth dependence of the critical angles in silicon along a ⟨111⟩ axis and a (110) plane.

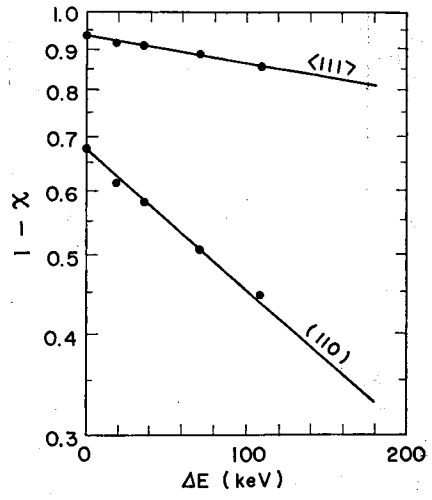

Fig. 8. Depth dependence of $(1-\chi)$ in silicon along a ⟨111⟩ axis and a (110) plane.

4.2. The Minimum Scattering Yield

According to Lindhard,[11] the minimum scatterking yield χ in a vibrating lattice is estimated to be

$$\chi = Nd\pi(a_{TF}^2+\langle u^2\rangle_{av}) \qquad \text{for axial,} \tag{12}$$

and

$$\chi = 2a_{TF}/d_p \qquad \text{for planar,} \tag{13}$$

where $\langle u^2\rangle_{av}$ is the mean-square amplitude of the lattice vibrations perpendicular to the axial channel. Equation (12) is correct only when the incident particle is scattered from the crystal surface, *i.e.* the scattering depth is equal to zero.

As for the value of $\langle u^2\rangle_{av}$ in silicon at room temperature, $\langle u^2\rangle_{av}^{1/2}=0.076$ Å.[16] In addition, $N=5.21\times10^{22}$ cm^{-3} in silicon. Thus the theoretical values of χ in

$\langle 111 \rangle$ axial and (110) planar channels of a silicon crystal are χ (theoretical) $=0.024$ and 0.17, respectively. The observed value of χ is obtained from Fig. 3 and Fig. 6. It is important that the observed value of χ has a depth dependence. Fig. 8 illustrates the depth dependence of $(1-\chi)$ as a function of ΔE. The extrapolation method determines the experimental value of χ at $\Delta E=0$ as χ (experimental) $=0.07$ for the $\langle 111 \rangle$ axial case, and 0.32 for the (110) planar case. Thus we find that χ (experimental) agrees fairly well with χ (theoretical). The observed value is slightly larger than the predicted one, because of the other causes such as imperfections of the crystal surface and multiple scattering of protons.

4.3. Analysis of the Energy Spectra

The relationship between the fraction $f_c(x)$ of particles in the channeling mode at the scattering depth x has been found experimentally by Andersen et al.:[12]

$$f_c(x) = f_c(0) \exp\left(-\frac{x}{\Lambda_c \cos\theta_1}\right), \tag{14}$$

where Λ_c is the mean distance that a proton travels in the channeling mode before being back-scattered. The channeling probability $f_c(m)$ corresponding to a given channel number m of P.H.A. is written as

$$f_c(m) = 1-\frac{N_{mc}}{N_{mr}}, \tag{15}$$

where N_{mc} and N_{mr} are the normalized yield at m channels of the energy spectra for the aligned and random beams, respectively.

Fig. 9 illustrates the experimental values of $f_c(m)$ calculated from eq. (15) as a function of m. In this analysis, the finite energy resolution and the energy straggling of the protons in silicon are neglected. Thus the extrapolated values of $f_c(m)$ at the surface of the crystal are 0.93 and 0.66, so that the channeling probability of the protons near the clean surface should be 93% and 66% for the $\langle 111 \rangle$ axial and the (110) planar channeling, respectively. As a matter of course, these results agree well with those obtained in the previous considerations about χ.

Fig. 6 shows that the shoulder parts become extremely remarkable as the scattering depth (*i.e.* ΔE) is reduced. From this fact together with the analysis of critical angles and minimum scattering yield mentioned above, we find that the channeling phenomena in the present energy region is dominated by the interaction of incident ions with the surface layer of the crystal. It should be noted in Fig. 2 that there is a conspicuous hump near the maximum energy ($\sim$175 keV) in the energy spectrum at the shoulder part. It is clear that this hump is not due to the imperfections or contaminations at the crystal surface, because there is no such

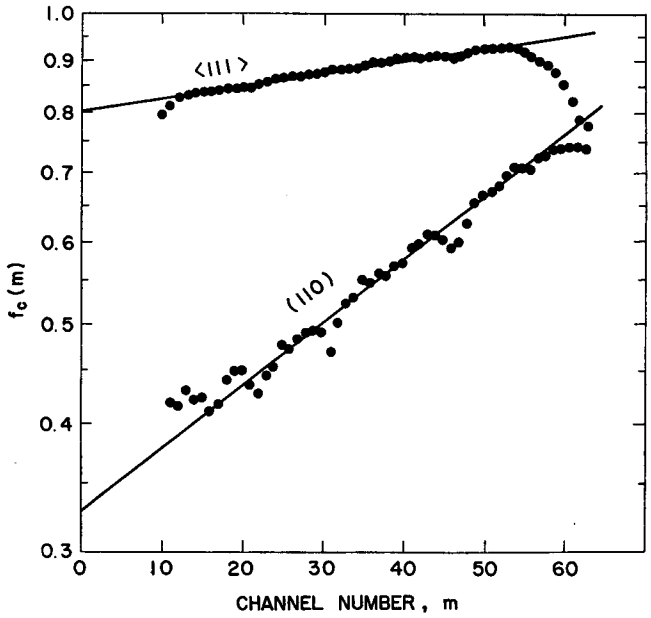

Fig. 9. The values of $f_c(m)$ as a function of m on a log-linear plot calculated from eq. (15).

hump in the spectra at the random and channeling directions. Therefore, the closer study on the hump of the energy spectrum at the shoulder part is valuable to clarify the detailed mechanism of the channeling phenomena.

Acknowledgements

We would like to thank Messrs. Y. Goto and M. Mizobuchi for help with the experiments.

References

1) G.R. Piercy, M. McCargo, F. Brown and J.A. Davies: Phys. Rev. Letters, **10**, 399 (1963), Canad. J. Phys., **42**, 1116 (1964).
2) R.S. Nelson and M.W. Thompson: Phil. Mag., **8**, 1677 (1963).
3) H. Lutz and R. Sizmann: Phys. Letters, **5**, 113 (1963).
4) E. Bøgh and E. Uggerhøj: Nucl. Instrum. Meth., **38**, 216 (1965).
5) C. Ellegaard and N.O. Lassen: K. Danske Vidensk. Selsk. mat.-fys. Medd., **35**, No. 16 (1967).
6) J.A. Davies, J. Denhartog, L. Eriksson and J.W. Mayer: Canad. J. Phys., **45**, 4053 (1967).
7) D.W. Palmer and E. d'Artmare: Phil. Mag., **17**, 1195 (1968).
8) R. Behrisch: Canad. J. Phys., **46**, 527 (1968).
9) S.T. Picraux, J.A. Davies, L. Eriksson, N.G.E. Johansson and J.W. Mayer: Phys. Rev., **180**, 873 (1969).
10) J.A. Davies, L. Eriksson, N.G.E. Johansson and I.V. Mitchell: Phys. Rev., **181**, 548 (1969).

11) J. Lindhard: K. Danske Vidensk. Selsk. mat.-fys. Medd., **34**, No. 14 (1965).
12) J.U. Andersen, J.A. Davies, K.O. Nielsen and S.L. Andersen: Nucl. Instrum. Meth., **38**, 210 (1965).
13) D.A.S. Walker and L.E. McGann: Nucl. Instrum. Meth., **62**, 228 (1968).
14) A.R. Sattler and G. Dearnaley: Phys. Rev., **161**, 244 (1967).
15) J.A. Davies, J. Denhartog and J.L. Whitton: Phys. Rev., **165**, 345 (1968).
16) C. Erginsoy: Phys. Rev. Letters, **15**, 360 (1965).